Open Access
Asian-Australas J Anim Sci
Vol. 31, No. 6:791-797 June 2018
https://doi.org/10.5713/ajas.17.0744
pISSN 1011-2367 eISSN 1976-5517

AJAS
Asian-Australasian Journal of Animal Sciences

A demonstration of the H3 trimethylation ChIP-seq analysis of galline follicular mesenchymal cells and male germ cells

Kaj Chokeshaiusaha[1], Denis Puthier[2], Catherine Nguyen[2], and Thanida Sananmuang[1,*]

* **Corresponding Author:** Thanida Sananmuang
Tel: + 66-38358137, **Fax:** +66-38358141,
E-mail: t.sananmuang@gmail.com

[1] Faculty of Veterinary Medicine, Rajamangala University of Technology Tawan-OK 43 Moo 6 Bangpra, Sriracha Chonburi 20110, Thailand
[2] Laboratoire TAGC/INSERM U1090, Parc Scientifique de Luminy case 928, 163, avenue de Luminy, Marseille cedex 09 13288, France

ORCID
Kaj Chokeshaiusaha
https://orcid.org/0000-0002-2953-9101
Denis Puthier
https://orcid.org/0000-0002-7240-5280
Catherine Nguyen
https://orcid.org/0000-0001-9376-6360
Thanida Sananmuang
https://orcid.org/0000-0002-8653-3558

Submitted Oct 9, 2017; Revised Nov 23, 2017; Accepted Jan 10, 2018

Objective: Trimethylation of histone 3 (H3) at 4th lysine N-termini (H3K4me3) in gene promoter region was the universal marker of active genes specific to cell lineage. On the contrary, coexistence of trimethylation at 27th lysine (H3K27me3) in the same loci—the bivalent H3K4m3/H3K27me3 was known to suspend the gene transcription in germ cells, and could also be inherited to the developed stem cell. In galline species, throughout example of H3K4m3 and H3K27me3 ChIP-seq analysis was still not provided. We therefore designed and demonstrated such procedures using ChIP-seq and mRNA-seq data of chicken follicular mesenchymal cells and male germ cells.
Methods: Analytical workflow was designed and provided in this study. ChIP-seq and RNA-seq datasets of follicular mesenchymal cells and male germ cells were acquired and properly preprocessed. Peak calling by Model-based analysis of ChIP-seq 2 was performed to identify H3K4m3 or H3K27me3 enriched regions (Fold-change≥2, FDR≤0.01) in gene promoter regions. Integrative genomics viewer was utilized for cellular retinoic acid binding protein 1 (*CRABP1*), growth differentiation factor 10 (*GDF10*), and gremlin 1 (*GREM1*) gene explorations.
Results: The acquired results indicated that follicular mesenchymal cells and germ cells shared several unique gene promoter regions enriched with H3K4me3 (5,704 peaks) and also unique regions of bivalent H3K4m3/H3K27me3 shared between all cell types and germ cells (1,909 peaks). Subsequent observation of follicular mesenchyme-specific genes—*CRABP1*, *GDF10*, and *GREM1* correctly revealed vigorous transcriptions of these genes in follicular mesenchymal cells. As expected, bivalent H3K4m3/H3K27me3 pattern was manifested in gene promoter regions of germ cells, and thus suspended their transcriptions.
Conclusion: According the results, an example of chicken H3K4m3/H3K27me3 ChIP-seq data analysis was successfully demonstrated in this study. Hopefully, the provided methodology should hereby be useful for galline ChIP-seq data analysis in the future.

Keywords: ChIP-seq; Follicular Mesenchymal Cell; Galline; Germ Cell; Histone 3 Trimethylation

INTRODUCTION

Functional cells of multi-cellular organisms maintain their mutual state by adopting specific gene expression patterns. They hereby fix their transcriptional activities by imprinting a particular chromatin structure into genome to allocate and control target gene regions—also recognized as the chromatin packaging [1]. In eukaryotic cell, a chromatin consists of several units of 147 base pairs DNA twining around nucleosome formed by histone octamer—which is the molecule responsible for the chromatin packaging process. A histone octamer comprised of four basic core histones—H2A, H2B, H3, and H4 which are targets for histone modification—methylation, phosphorylation and acetylation. When a precursor cell is committed a lineage-specific development, it modifies particular N-termini amino acids of

Copyright © 2018 by Asian-Australasian Journal of Animal Sciences
This is an open-access article distributed under the terms of the Creative Commons Attribution Non-Commercial License (http://creativecommons.org/licenses/by-nc/4.0/), which permits unrestricted non-commercial use, distribution, and reproduction in any medium, provided the original work is properly cited.

specific core histones. This event thus results in chromatin packaging to control gene a transcription pattern specific to its lineage-committed cell [1,2].

Different histone modification can relax or condense chromatin structures differently. Since each specific chromatin structure can affect the accessibility of gene transcription factors and RNA polymerase II differently at a gene promoter region, they will result in a gene transcription pattern specific to the lineage-committed cell [1-3]. Among well-recognized histone modifications, trimethyl modification of histone 3 (H3) at 4th lysine N-termini (H3K4me3) is very common in active gene transcriptions of several lineage-committed cells [4,5]. This phenomenon, however cannot conclusively comply with several genes in stem cells and germ cells, of which H3K4me3 regions are presented without transcription. Interestingly, such genes always demonstrate not only trimethylation of H3 on 4th lysine (H3K4me3), but also the 27th lysine (H3K27me3) in the same loci of N-termini—the bivalent H3K4m3/H3K27me3 chromatin or poised chromatin [2,6,7].

In the embryonic stem cells, the presence of H3K4me3 in the poised gene helps marking the gene as the active one. However, the concurrent H3K27me3 repressed the transcription and thus guarantees the cells' pluripotent state [6,7]. Actually, such characteristics were proved to be inherited from germ cells even prior to fertilization. According to this reason, the study of H3K4me3/H3K27me3 bivalent (poised) epigenetic state in male germ cells became a very popular topic in epigenetic evolution studies [2,8].

Chromatin immunoprecipitation (ChIP) assays with sequencing or ChIP-Seq is a sequencing technology generally utilized to study genome-wide H3 trimethylation—H3K4me3 and H3K27me3. In ChIP-Seq, the chromatin regions presented with modified histones of interest are immunoprecipitated and sequenced to study epigenetic control of gene expressions in several cell types [2,5,9,10]. Not only mammals, ChIP-Seq of H3 trimethylation were also conducted in chicken (*Gallus gallus*) as the representative of galline species [2,11-13]. These studies provided biologists and veterinarians the valuable insights into evolution and cell development of galline species. Of note, an increase of H3K4me3 and H3K27me3 ChIP-seq databases in chicken also allowed both biologists and veterinarians a new opportunity to observe and meta-analyze ChIP-seq data of various cell types acquired from different experiments.

Analytical guidelines are generally concerned in human and mouse ChIP-Seq studies [10]. On the contrary, the issue was limitedly described in H3 trimethylation ChIP-Seq data analysis in galline species [2,12,13]. Since the procedures could affect the analytical results differently, a practical demonstration of such approach should prove beneficial, especially for those who are not acquainted with ChIP-Seq data analysis. Due to such necessity, we therefore demonstrated a chicken ChIP-seq meta-analysis in this study. The H3K4me3 ChIP-Seq data of chicken follicular mesenchymal cells and male germ cells were acquired, and we also included H3K27me3 ChIP-Seq data of chicken germ cells to demonstrate the effect of bivalent H3K4me3/H3K27me3 on gene transcription.

MATERIALS AND METHODS

Sample datasets

As far as we knew, the follicular mesenchymal cell was the only lineage-committed cell type with H3 trimethylation ChIP-seq data available in public database. A list of follicular mesenchymal cell and germ cell datasets used in this study is provided (Table 1). Follicular mesenchymal cells used in this study consisted of two populations isolated from median (Med) and lateral mesenchyme (Lat) of feather follicles, accordingly. Male germ cells used in this study derived from two time points during development: pachytene spermatocyte (PS) acquired

Table 1. Raw data files used in this study

Cell type's abbreviation	Description	Sample file	Control file
PS_K4	ChIP-seq of H3K4me3 of pachytene spermatocye	SRR1977505	SRR1977507
PS_K27	ChIP-seq of H3K27me3 of pachytene spermatocyte	SRR1977506	SRR1977507
PS_RNA-seq	RNA-seq of pachytene spermatocyte	SRR1977509	-
RS_K4	ChIP-seq of H3K4me3 of round spermatid	SRR1977535	SRR1977537
RS_K27	ChIP-seq of H3K27me3 of round spermatid	SRR1977536	SRR1977537
RS_RNA-seq	RNA-seq of round spermatid	SRR1977540	-
Lat_K4(1)	ChIP-seq of H3K4me3 of lateral mesenchyme	SRR4125205	SRR4125207
Lat_RNA-seq(1)	RNA-seq of lateral mesenchyme	SRR4125190	-
Med_K4(1)	ChIP-seq of H3K4me3 of medial mesenchyme	SRR4125206	SRR4125208
Med_RNA-seq(1)	RNA-seq of medial mesenchyme	SRR4125192	-
Lat_K4(2)	ChIP-seq of H3K4me3 of lateral mesenchyme	SRR4125209	SRR4125211
Lat_RNA-seq(2)	RNA-seq of lateral mesenchyme	SRR4125191	-
Med_K4(2)	ChIP-seq of H3K4me3 of medial mesenchyme	SRR4125210	SRR4125212
Med_RNA-seq(2)	RNA-seq of medial mesenchyme	SRR4125193	-

during prophase of meiosis I, and round spermatid (RS) acquired after completing meiosis. Both germ cell types were representatives of male germ cells to illustrate the poised genes—where their poised states were already known to be retained throughout spermatogenic development [2]. For ChIP-seq data, the sample file and its corresponding control file were provided together. Of note, the control file was not required for RNA-seq data analyses, and thus not provided.

Analytical workflow

In this study, we categorized our analytical processes into 3 steps—data preprocessing, peak calling with visualization, and integrative genomics viewer (IGV) exploration (Figure 1). In brief, the sample datasets would be aligned to chicken genome in order to acquire ChIP files and RNA-seq files in the data preprocessing step (Figure 1A). The ChIP files were then applied in peak calling step to identify genome regions enriched with H3 trimethylation—the significant peaks (Figure 1B). Only peaks overlapped with gene promoter region would be considered in IGV exploration of which, the enriched peaks along with the mapped sequences ChIP and RNA-seq files were integrated and visualized together in IGV platform (Figure 1C).

Data preprocessing: The sequence read archive (SRA) files of germ cells and follicular mensenchymal ChIP-Seq and RNA-Seq datasets were retrieved from SRA database (https://www.ncbi.nlm.nih.gov/sra) (Table 1), subsequently extracted, and preprocessed as previously described [14]. The ChIP files were aligned to chicken genome (*Gallus gallus* 5.0) by Bowtie2 aligner [15], while STAR aligner was applied with the RNA-seq files [14,16]. The aligned files were converted into "bam" format, indexed by gene annotation, removed for duplicated sequences [17], and bias corrected for guanine-cytosine base balance [18] to acquire ChIP files and RNA-seq files. The qualities of both raw and preprocessed datasets were then determined by FastQC as previously described [14]. For ChIP quality determination, normalized strand cross-correlation coefficient (NSC), relative strand cross-correlation coefficient (RSC) and DNA fragment length were additionally included. In more details, NSC is genome-wide correlation between positive and negative strand read counts when shifted by half of the fragment length relative to background. NSC value thus represents enrichment of clustered ChIP fragments around target sites. RSC is the relative enrichment of fragment-length cross-correla-

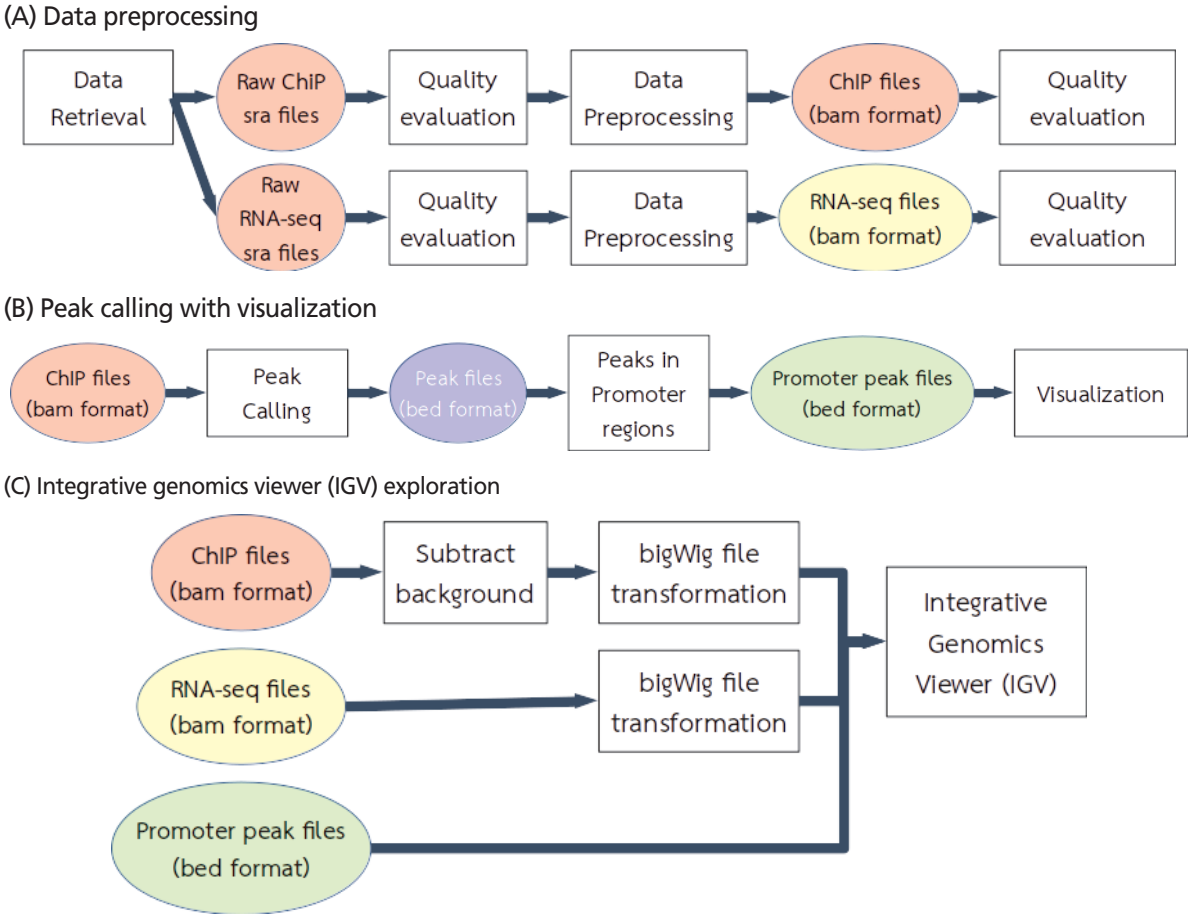

Figure 1. Analytical workflow for this study. Analytical processes were categorized into 3 steps—data preprocessing (A), peak calling with visualization (B), and integrative genomics viewer (IGV) exploration (C). The files required and outcome for each analytical step are provided.

tion to read-length cross-correlation. The RSC thus represented the clustering of relatively fixed sized fragment around target sites.

Peak calling with visualization: Peak calling was, in case of this study, the computational method to identify genome-wide chromatin regions with targeted H3 trimethylation significant to the other regions. The peaks therefore represented the genome area with significant presences of H3K4me3 or H3K27me3 when compared to the same region presented in the corresponding control datasets (Table 1). Model-based analysis of ChIP-seq 2 (MACS2) algorithm [19] was used in this study. Since the broad peak regions were suggested in the previous quality analysis, we applied broad peak calling function in MACS2 with all ChIP files. Further details for such function calling was already described [19]. Significant peaks were those with false discovery rate (FDR) ≤0.01 and Fold-change ≥2 presented with chicken gene promoter regions (2,000 base pairs upstream to 200 base pairs downstream of gene promoter) (Peak files in Figure 1B). Peak files were also utilized for counting aggregated DNA within peak region, and counting the DNA fragments distributed from the transcription start site of chicken genes (Figure 2B).

Integrative genomics viewer (IGV) exploration: The peak files along with their corresponding ChIP files and RNA-seq files were integratively observed together in IGV platform (Figure 1C). The Gal_gal5.0 genome (UCSC version galGal5

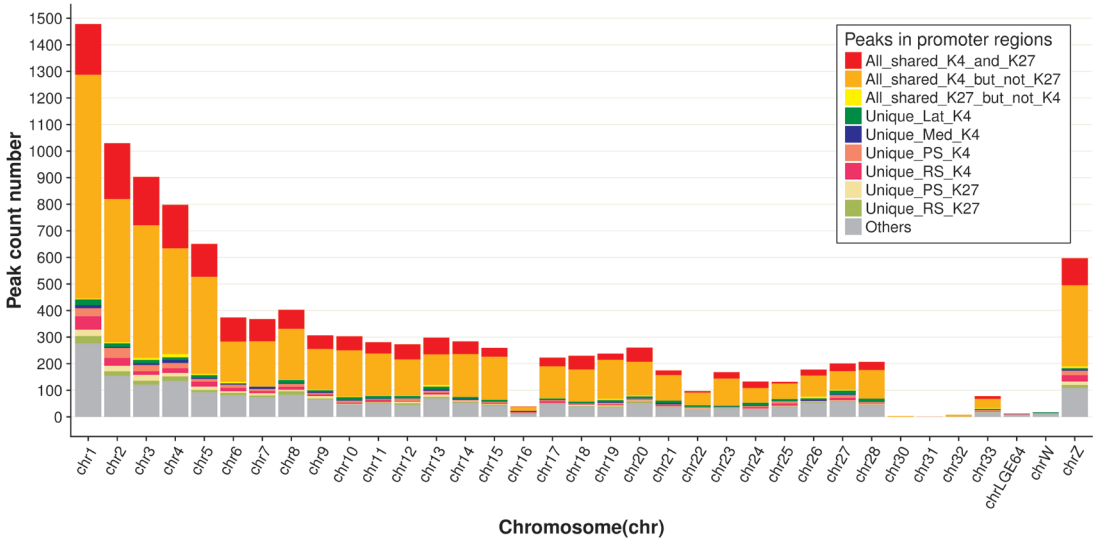

(A)

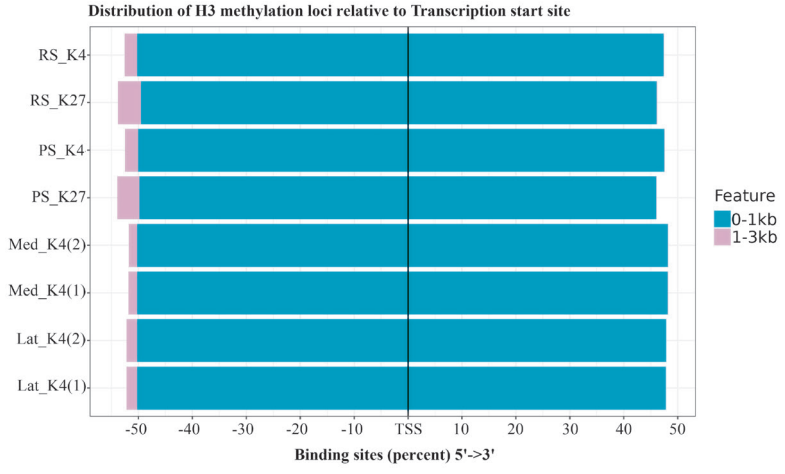

(B)

Figure 2. H3 trimethylation loci. The total number of peaks significantly identified were categorized according to their regional chromosomes (A). Each color bar presented in the legend was described as following: ■, peaks shared among all samples with either K4 or K27 trimethylation (All_shared_K4_and_K27); ■, peaks presented only among samples with K4 trimethylation (All_shared_K4_but_not_K27); ■, peaks presented only among samples with K27 trimethylation (All_shared_K27_but_not_K4); ■, peaks presented only in Lat_K4 (Unique_Lat_K4); ■, peaks presented only in Med_K4 (Unique_Med_K4); ■, peaks presented only in PS_K4 (Unique_PS_K4); ■, peaks presented only in RS_K4 (Unique_RS_K4); ■, peaks presented only in PS_K27 (Unique_PS_K27); ■, peaks presented only in RS_K27 (Unique_RS_K27), and ■, other peaks not in the previously mentioned groups. Distribution of precipitated DNA fragments acquired from sample ChIP-seq data according to chicken gene transcription start site was also demonstrated (B). Aggregation of fragments within 0-1 kilobases (■) and 1-3 kilobases (■) are presented.

released in December 2015) was administrated as the reference genome. The gal_Gal5.0 consisted of 34 chromosomes, 1 linkage group and 15,411 unplaced scaffolds. Further details of IGV platform can be acquired online (http://software.broadinstitute.org/software/igv/). In brief, DNA aggregations along the genome of sample ChIP files were expressed by blue heatmap. Similarly, the density of transcript fragments from RNA-seq files acquired from the corresponding cell sample were expressed by red heatmap. Peak regions of each cell type were also included in the figure the aggregated DNA fragments from ChIP files. To demonstrate bivalent H3K4me3/H3K27me3 chromatin of germ cell samples, cellular retinoic acid binding protein 1 (*CRABP1*), growth differentiation factor 10 (*GDF10*), and gremlin 1 (*GREM1*) genes were chosen for illustration (Figure 4). We select such genes due to the fact that transcription of these genes was crucial in topological control of chicken feather's generation of follicular mesenchyme [11].

RESULTS

All sample datasets were successfully preprocessed and aligned to chicken genome

The raw datasets of all cell types were retrieved and preprocessed according to the methodology (Figure 1A). All preprocessed datasets (both ChIP-seq and RNA-seq data in Table 1) acquired quality scores across all bases ≥30 without presence of contaminated adapters. Alignment percentages of ChIP-seq and RNA-seq datasets were ≥85% and ≥70%, accordingly. NSC, RSC, and DNA fragment length of ChIP-seq samples are provided in Table 2.

Follicular mesenchymal cells and germ cells shared several gene promoter regions with H3K4me3 and H3K27me3

As previously described in materials and methods, the peaks were the chromatin loci in gene promoter regions enriched with target H3 trimethylations (H3K4me3 or H3K27me3). When categorized the acquired peaks according to their localized chromosomes, chromosome 1 contained the largest number of peaks comparing to the others (chr1 in Figure 2A).

Table 2. NSC values, RSC values, and DNA fragment length of ChIP-seq samples

Cell type	Sample file	NSC	RSC	Fragment length
PS_K4	SRR1977505	1.10	1.05	170
PS_K27	SRR1977506	1.02	1.28	170
RS_K4	SRR1977535	1.13	1.10	170
RS_K27	SRR1977536	1.03	1.25	170
Lat_K4_1	SRR4125205	1.02	0.72	210
Med_K4_1	SRR4125206	1.01	0.64	200
Lat_K4_2	SRR4125209	1.02	0.71	240
Med_K4_2	SRR4125210	1.01	0.66	195

NSC, normalized strand cross; RSC, relative strand cross.

Most of aggregated DNA fragments of ChIP files were found distributed within 0-1 kilobases from the transcription start sites in all cell types (Figure 2B). The results indicated that that most H3K4me3 peaks (5,704 peaks) were uniquely shared among follicular mesenchymal cells and germ cells (lat_K4, med_K4, PS_K4, and RS_K4), and the second largest intersected peaks were uniquely shared among all H3K4me3 and H3K27me3 (1,909 peaks) (Figure 2A, 3).

CRABP1, *GDF10*, and *GREM1* genes of chicken germ cells adopted the bivalent H3 trimethylation chromatin pattern with presence of transcription's inhibition

Follicular mesenchymal cells (Lat RNA-seq and Med RNA-seq in Figure 4) expressed *CRABP1*, *GDF10*, and *GREM1* genes higher than germ cells (PS RNA-seq and RS RNA-seq in Figure 4). Of note, the bivalent H3K4me3/H3K27me3 pattern near transcription start site of these gene in germ cells was demonstrated by the significant peak regions (PS_K4 Peak, PS_K27 Peak, RS_K4 Peak, and RS_K27 Peak in Figure 4) with presence of remarkable ChIP-seq DNA aggregations (PS_K4 ChIP-seq, PS_K27 ChIP-seq, RS_K4 ChIP-seq, and RS_K27 ChIP-seq in Figure 4).

DISCUSSION

Data quality was among the most critical issues in ChIP-seq analysis due to its later effect on measurement and comparison. According to this reason, we preprocessed the ChIP-seq data to acquire adequate quality and alignment percentages. Another crucial issue in ChIP-seq quality was the determination of signal-to-noise ratio represented by NSC and RSC values. ChIP-seq data with few genuine binding site regions usually rendered high NSC (≥1.5) and RSC (≥0.8), accordingly. However, marks that tend to be enriched at repeat-like regions with diffused genome-wide patterns like H3 trimethylation usually show lower NSC and RSC values—which also presented in our study [10,11] (Table 2).

Since H3 trimethylation (H3K4me3 or H3K27me3) at gene promoter regions were strongly associated with gene transcription control [4,5,12], only peaks within gene promoter region were hereby considered in this study. Inheritance mechanism of H3K4me3/H3K27me3 bivalent state from germ cells to embryonic stem cells, and activation mechanism of lineage-specific genes in lineage-committed cells were comprehensively described elsewhere [20], and are not included in this discussion. According to the result, most H3 trimethylation peaks in both follicular mesenchymal cells and germ cells were located in chromosome 1—agreeing with the largest gene numbers in the chromosome (2,162 coding genes and 524 non-coding genes) (chr1 in Figure 2). Interestingly, the largest number of intersected H3K4me3 peaks among ChIP-seq samples (orange bar in Figure 3) implied the conserved

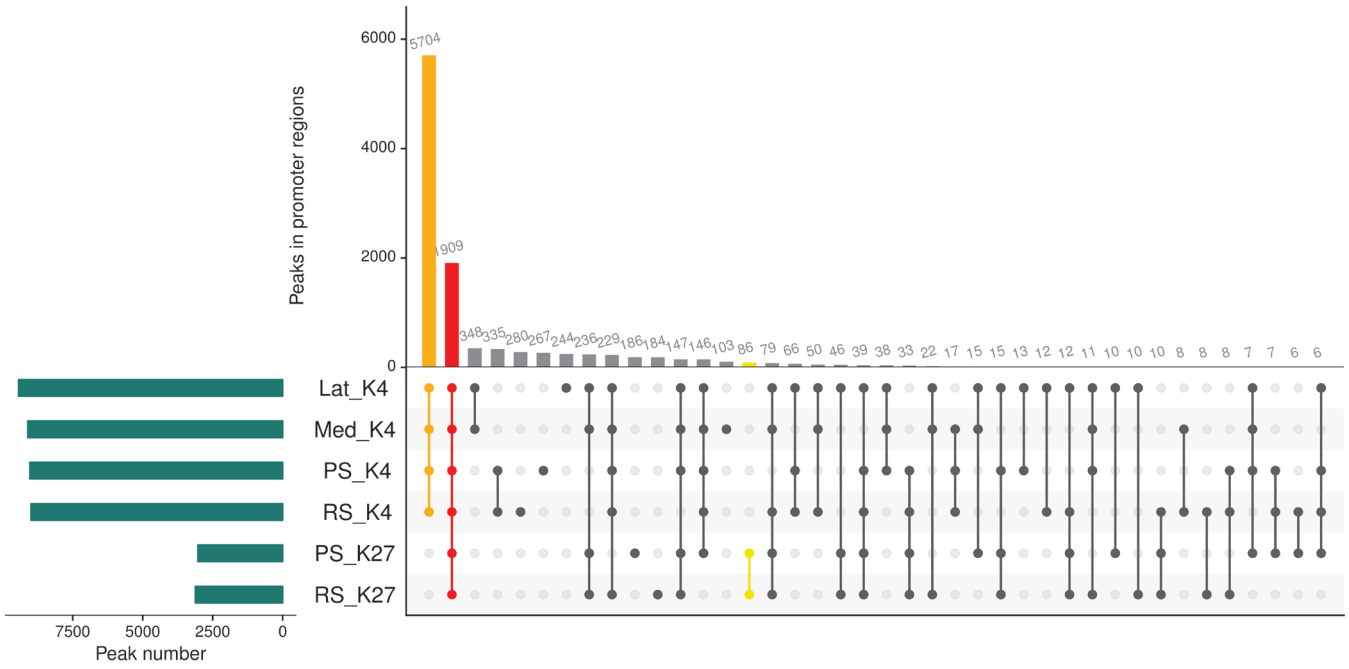

Figure 3. UpSet plot of intersected peaks among cell types. The intersected peaks shared among cell types (Lat_K4, Med_K4, PS_K4, RS_K4, PS_K27, and RS_K27) were presented by UpSet plot. The connected lines among cell types shown in the lower panel of the plot represented the group of intersected peaks among them. The upper panel bar graph of the plot presented the number of peaks found in each group. The shared peak number among all samples with either K4 or K27 trimethylation and only K4 trimethylation are in red (■) and orange (■) color, accordingly. The horizontal leftmost bar graph (olive green color, ■) show to total number of peaks presented in each cell type.

role of H3K4me3 among chicken germ cells and mesenchymal cells. Of note, shared presented among H3K4me3 and H3K27me3 (red bar in Figure 3) could only partially imply several unique genes controlled by H3K4me3/H3K27me3

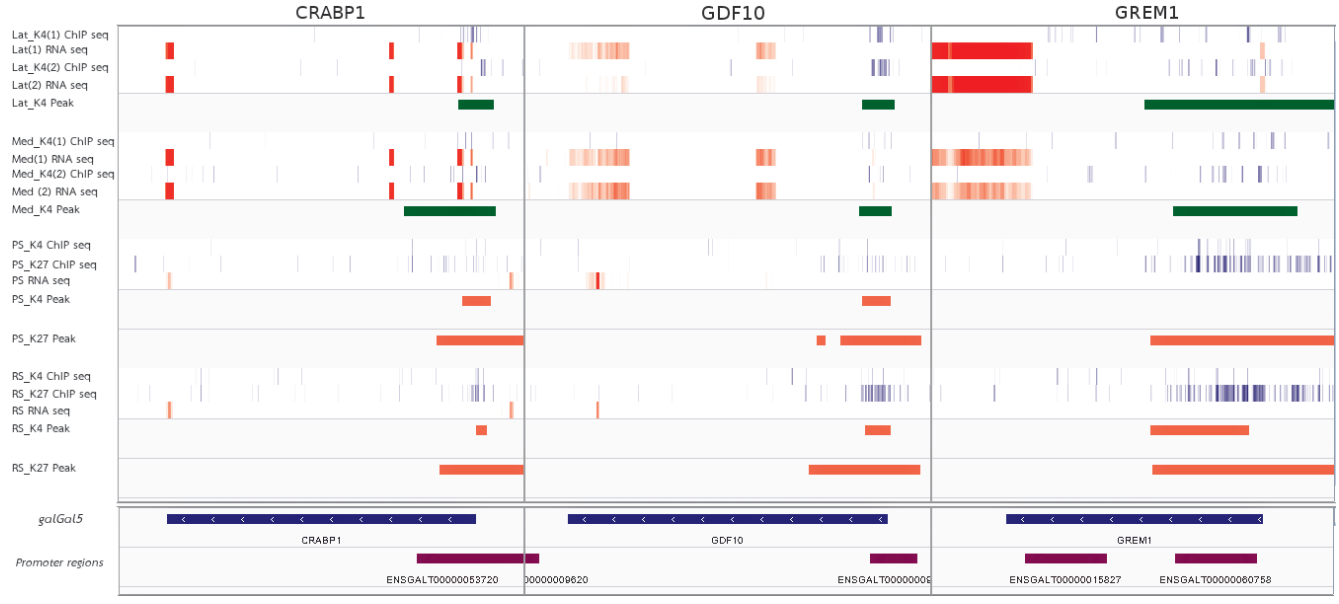

Figure 4. Chromatin histone 3 (H3) trimethylation state and transcription of cellular retinoic acid binding protein 1 (*CRABP1*), growth differentiation factor 10 (*GDF10*), and gremlin 1 (*GREM1*) genes. The heatmaps of *CRABP1*, *GDF10*, and *GREM1* genes were acquired from the integrative genomics viewer (IGV) interface. The chicken full genome sequences was used to identify the chromatin loci of these genes with transcription direction indicated by the arrow heads presented in the genome along with the associated promoters in the area (galGal5 and Promoter regions at the bottom of the figure). The figure show 3 types of data—ChIP-seq, RNA-seq, and Peak files acquired from each sample cell type. In brief, ChIP-seq data show the density of DNA fragments aligned to a chromatin region (aggregated DNA fragments) in blue heatmap. The RNA-seq data show the density of transcript fragments aligned to the gene regions representing level of gene expressions by red heatmap. Finally, the peak file of each cell sample indicated the chromatin region with significant peaks identifed by peak calling analysis.

bivalent state in chicken germ cells due to the lack of H3K-27me3 ChIP-Seq datasets from analysis.

To demonstrate the effect of H3K4me3/H3K27me3 bivalent state on transcription inhibition of germ cells [2,7], we chose *CRABP1*, *GDF10*, and *GREM1* as candidate genes due to their redundant lineage-specific transcriptions in follicular mesenchymal cells [11]. Visualization by IGV properly demonstrated such lineage-specific characteristics in follicular mesenchymal cells. On the contrary, inhibition of the gene transcription was obvious in germ cells with a significant presence of H3K4me3/H3K27me3 (poised) in the gene promoter regions as expected (Figure 4). As described in the introduction, such a poised state of genes in germ cells allowed them to inherit pluripotency to the later developed embryonoic stem cells. The observatory procedure in this study hereby successfully demonstrated the inhibitory effect of H3K4me3/H3K27me3 bivalent (poised) state on follicular mesenchyme-specific genes in chicken germ cells. By mean of this, other poised genes of interest could also be observed by adopting the same approach.

In conclusion, the current study provided an example for H3 trimethylation ChIP-seq analysis of chicken (*Gallus gallus*) cells. Since the methodology required no specific process, ChIP-seq data of other histone modifications could also be analyzed using similar approach. There were, however some important limitations that should be noted in this study. These included the lack of H3K27me3 ChIP-seq data of follicular mesenchymal cells to confirm abortion of poised genes, and limited samples per cell type available for valid differential analysis [21]. Hopefully, the rapid growth of galline ChIP-seq database would allow us to demonstrate such analysis in our future study.

CONFLICT OF INTEREST

We certify that there is no conflict of interest with any financial organization regarding the material discussed in the manuscript.

ACKNOWLEDGMENTS

The current study was fully supported by Thailand Research Fund (TRF) through New Research Scholar Program (Grant No. TRG5880003).

REFERENCES

1. Feil R, Khosla S. Genomic imprinting in mammals: an interplay between chromatin and DNA methylation? Trends Genet 1999;15:431-5.
2. Lesch BJ, Silber SJ, McCarrey JR, Page DC. Parallel evolution of male germline epigenetic poising and somatic development in animals. Nat Genet 2016;48:888-94.
3. Waclawska A, Kurpisz M. Key functional genes of spermatogenesis identified by microarray analysis. Syst Biol Reprod Med 2012;58:229-35.
4. Guenther MG, Levine SS, Boyer LA, Jaenisch R, Young RA. A chromatin landmark and transcription initiation at most promoters in human cells. Cell 2007;130:77-88.
5. Zhang B, Zheng H, Huang B, et al. Allelic reprogramming of the histone modification H3K4me3 in early mammalian development. Nature 2016;537(7621):553-7.
6. Azuara V, Perry P, Sauer S, et al. Chromatin signatures of pluripotent cell lines. Nat Cell Biol 2006;8:532-8.
7. Mikkelsen TS, Ku M, Jaffe DB, et al. Genome-wide maps of chromatin state in pluripotent and lineage-committed cells. Nature 2007;448(7153):553-60.
8. Villar D, Berthelot C, Aldridge S, et al. Enhancer evolution across 20 mammalian species. Cell 2015;160:554-66.
9. Eissenberg JC, Shilatifard A. Histone H3 lysine 4 (H3K4) methylation in development and differentiation. Dev Biol 2010;339:240-9.
10. Landt S, Marinov G. ChIP-seq guidelines and practices of the ENCODE and modENCODE consortia. Genome Res 2012;22:1813-31.
11. Li A, Figueroa S, Jiang T-X, et al. Diverse feather shape evolution enabled by coupling anisotropic signalling modules with self-organizing branching programme. Nat Commun 2017;8: ncomms14139.
12. Jahan S, Xu W, He S, et al. The chicken erythrocyte epigenome. Epigenetics Chromatin 2016;9:19.
13. Luo J, Mitra A, Tian F, et al. Histone methylation analysis and pathway predictions in chickens after MDV infection. PLoS One 2012;7:e41849.
14. Chokeshaiusaha K, Thanawongnuwech R, Puthier D, Nguyen C. Inspection of C-type lectin superfamily expression profile in chicken and mouse dendritic cells. Thai J Vet Med 2016;46: 443-53.
15. Langmead B, Salzberg SL. Fast gapped-read alignment with Bowtie 2. Nat Methods 2012;9:357-9.
16. Dobin A, Davis CA, Schlesinger F, et al. STAR: Ultrafast universal RNA-seq aligner. Bioinformatics 2013;29:15-21.
17. Li H, Handsaker B, Wysoker A, et al. The sequence alignment/map format and SAMtools. Bioinformatics 2009;25:2078-9.
18. Ramírez F, Dündar F, Diehl S, Grüning BA, Manke T. Deep Tools: A flexible platform for exploring deep-sequencing data. Nucleic Acids Res 2014;42 (Web Server issue):W187-91.
19. Feng J, Liu T, Qin B, Zhang Y, Liu XS. Identifying ChIP-seq enrichment using MACS. Nat Protoc 2012;7:1728-40.
20. Vastenhouw NL, Schier AF. Bivalent histone modifications in early embryogenesis. Curr Opin Cell Biol 2012;24:374-86.
21. Ross-Innes CS, Stark R, Teschendorff AE, et al. Differential oestrogen receptor binding is associated with clinical outcome in breast cancer. Nature 2012;184(7381):389-93.